

Substrate doping: A strategy for enhancing reactivity on gold nanocatalysts by tuning sp bands

Nisha Mammen, Stefano de Gironcoli, and Shobhana Narasimhan

Citation: *The Journal of Chemical Physics* **143**, 144307 (2015); doi: 10.1063/1.4932944

View online: <http://dx.doi.org/10.1063/1.4932944>

View Table of Contents: <http://scitation.aip.org/content/aip/journal/jcp/143/14?ver=pdfcov>

Published by the [AIP Publishing](#)

Articles you may be interested in

[Modifying ceria \(111\) with a TiO₂ nanocluster for enhanced reactivity](#)

J. Chem. Phys. **139**, 184710 (2013); 10.1063/1.4829758

[A DFT study of the NO dissociation on gold surfaces doped with transition metals](#)

J. Chem. Phys. **138**, 074701 (2013); 10.1063/1.4790602

[Oxidation of Al doped Au clusters: A first principles study](#)

J. Chem. Phys. **130**, 234309 (2009); 10.1063/1.3149849

[Charge redistribution in core-shell nanoparticles to promote oxygen reduction](#)

J. Chem. Phys. **130**, 194504 (2009); 10.1063/1.3134684

[O₂ evolution on a clean partially reduced rutile TiO₂ \(110\) surface and on the same surface precovered with Au₁ and Au₂: The importance of spin conservation](#)

J. Chem. Phys. **129**, 074705 (2008); 10.1063/1.2956506



AIP | APL Photonics

APL Photonics is pleased to announce
Benjamin Eggleton as its Editor-in-Chief



Substrate doping: A strategy for enhancing reactivity on gold nanocatalysts by tuning *sp* bands

Nisha Mammen,¹ Stefano de Gironcoli,² and Shobhana Narasimhan¹

¹Theoretical Sciences Unit, Jawaharlal Nehru Centre for Advanced Scientific Research, Jakkur, Bangalore 560064, India

²SISSA, via Bonomea 265, 34136 Trieste, Italy

(Received 1 April 2015; accepted 29 September 2015; published online 12 October 2015)

We suggest that the reactivity of Au nanocatalysts can be greatly increased by doping the oxide substrate on which they are placed with an electron donor. To demonstrate this, we perform density functional theory calculations on a model system consisting of a 20-atom gold cluster placed on a MgO substrate doped with Al atoms. We show that not only does such substrate doping switch the morphology of the nanoparticles from the three-dimensional tetrahedral form to the two-dimensional planar form, but it also significantly lowers the barrier for oxygen dissociation by an amount proportional to the dopant concentration. At a doping level of 2.78%, the dissociation barrier is reduced by more than half, which corresponds to a speeding up of the oxygen dissociation rate by five orders of magnitude at room temperature. This arises from a lowering in energy of the *s* and *p* states of Au. The *d* states are also lowered in energy, however, this by itself would have tended to reduce reactivity. We propose that a suitable measure of the reactivity of Au nanoparticles is the difference in energy of *sp* and *d* states. © 2015 AIP Publishing LLC. [<http://dx.doi.org/10.1063/1.4932944>]

Catalysts work by decreasing the activation barrier for a chemical reaction to proceed. One of the challenges in designing better catalysts is to come up with newer catalysts which lower barriers further; a reduction of even a few percent can translate into significant speeding up of reaction rates. It is now well-established that gold is not noble in nanometer sizes¹ and can catalyze several reactions: most notably, the conversion of noxious carbon monoxide to carbon dioxide.^{2–8} This reaction is of great technological interest because of its utility in devices such as catalytic converters in automobiles and fuel cells.

As a result of the insights accumulated from a combination of experimental and theoretical work, it was realized that it should be possible to fine-tune the electronic (and hence catalytic) properties of gold clusters by controlling factors such as their size and shape, as well as by doping either the clusters themselves or the support on which they were placed.^{9,10} Indeed, recently it has been shown, both theoretically¹¹ and experimentally,^{12,13} that doping the oxide substrate on which gold nanocatalysts are supported, with an electron donor, can control the morphology of the nanoparticles. The truly interesting question is whether such substrate doping also improves catalytic properties. We now show, using first-principles density functional theory (DFT) calculations, and considering oxygen dissociation as a simple model reaction, that such doping can also significantly reduce reaction barriers, by an amount proportional to the doping concentration.

The representative system we choose to study, a 20-atom gold cluster placed on a MgO substrate, has been the subject of several previous studies.^{14–19} Au₂₀ has two low-energy isomers: a three-dimensional tetrahedral form (T) and a two-dimensional planar form (P). T is lower in energy in the gas phase as well as on pristine MgO; however, there is reason

to speculate that P, if it could be somehow stabilized, might be the better catalyst. One, therefore, looks for strategies to coax the system into favoring P over T. Previous authors had suggested two methods for this: using an ultra-thin MgO layer placed on a metal substrate,^{14–17} and placing the whole system in a high electric field.¹⁸

While these suggestions are of great fundamental interest, we recently demonstrated the efficacy of a third solution¹¹ which we believe might translate more easily to practical applications: doping the MgO substrate with a small fraction of impurity atoms. Upon doping with certain electron donors such as Al, the extra electrons are transferred to the gold cluster, which then prefers to flatten out. Al-doped MgO^{20,21} is one of the simplest substrates with which to model electron donation. Using DFT, we showed that when the Al doping concentration exceeded ~0.4%, P became energetically lower than T.¹¹ The strategy of substrate doping as a way of modifying Au nanoparticle morphologies has subsequently been shown to work experimentally, in this case using Mo (Cr) atoms as the electron donors, and CaO (MgO) as the substrate;^{12,13} this has recently been interpreted in terms of redox chemistry.²² Subsequently, it has also been shown theoretically that a similar effect can be achieved by depositing Au₂₀ on N-doped graphene²³ or on silicene supported on Ag(111).²⁴

Our spin-polarized DFT calculations have been performed using the Quantum-ESPRESSO package,²⁵ with ultrasoft pseudopotentials,²⁶ and a plane wave basis set, with cutoffs of 30 Ry and 240 Ry for wave functions and charge densities, respectively. Exchange-correlation interactions were treated using the PW91 form of the generalized gradient approximation.²⁷ The Au₂₀ cluster was placed on a 6 × 6 surface cell comprised of four layers of MgO; periodic boundary conditions were then used. In the surface-normal direction,

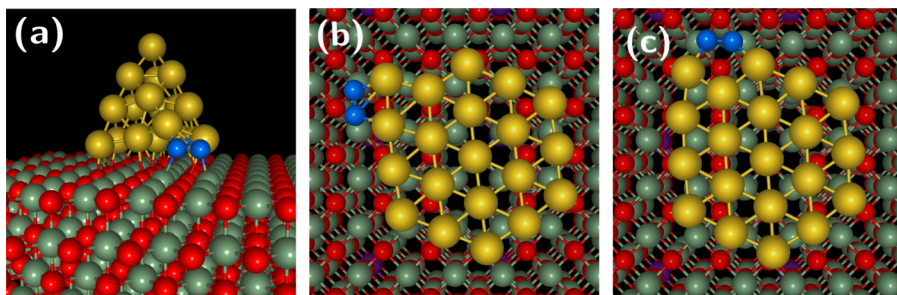


FIG. 1. Low-energy adsorption geometries for a single O_2 molecule adsorbed on a 20 atom gold cluster supported on MgO. (a) T1 for O_2 on Au(T)/MgO, (b) P1, and (c) P2 for O_2 on Au(P) on 2.78% Al-doped MgO. Gray, purple, and yellow spheres represent Mg, Al, and Au atoms, respectively. O atoms in the substrate/adsorbed on the surface are red/blue.

a vacuum spacing of ~ 14 Å was used. The Brillouin zone was sampled at the zone center only. All atomic coordinates were relaxed till forces were < 0.001 Ry/bohr.

To examine the effects of progressive substrate doping, we have considered four dopant concentrations: 0%, 0.69%, 1.39%, and 2.78%. The doping by an electron donor was modeled by substituting the appropriate number of sub-surface Mg atoms with Al. The dopant atoms were placed in the third layer from the surface, though the effects of changing the positions of dopant atoms were explored. In Fig. 1, we show the lowest energy configuration found by us for adsorption on the T cluster on pristine MgO (labeled T1), as well as two low-energy configurations for adsorption on the P cluster (labeled P1 and P2), on the 2.78% Al-doped MgO substrate. These geometries are in agreement with previous predictions for the favored adsorption sites on Au clusters on oxide substrates.^{4,28} In an actual experimental situation, several sites with differing barriers will be occupied, and one will see a combined effect.²⁹

We define the adsorption energy as $E_{\text{ads}} = -\{E_{\text{tot}}[(\text{Au}_{20} + \text{O}_2)/\text{MgO}] - E_{\text{tot}}(\text{Au}_{20}/\text{MgO}) - E_{\text{tot}}(\text{O}_2)\}$, where the terms on the right-hand-side are the total energies of, respectively (i) the system consisting of O_2 adsorbed on the Au_{20} cluster on a MgO substrate, (ii) just the Au_{20} on MgO, and (iii) O_2 in the gas phase; all these are computed in relaxed geometries. On the undoped MgO, the most favorable adsorption geometry on the planar cluster is P2, with $E_{\text{ads}} = 0.73$ eV; this configuration is lower in energy than the P1 geometry by 0.61 eV. However, at a doping concentration of 2.78%, P1 is the most stable adsorption geometry with $E_{\text{ads}} = 0.95$ eV, while the P2

geometry has $E_{\text{ads}} = 0.69$ eV. We note that substrate doping also has a significant effect on the binding of O_2 on the bare MgO substrate (i.e., when no Au clusters are present). It is unfavorable for O_2 to bind on bare undoped MgO; however, on bare 2.78% doped MgO, E_{ads} increases to the rather high value of 3.30 eV. It is important to note that this value is modified significantly when Au clusters are present on the doped surface, e.g., at 2.78% doping, the highest value of E_{ads} away from the cluster is found to be 0.59 eV. This may be compared with values of E_{ads} of 0.95 eV and 0.69 eV on the P1 and P2 sites, respectively, of the Au cluster, i.e., when Au clusters are present on doped MgO, we find that the O_2 molecule would prefer to bind to the Au cluster rather than to uncovered areas of the doped substrate.

Next, in order to obtain an indication of the impact that the substrate doping may have on chemical reactivity, we compute the dissociation barriers E_{diss} of a single molecule of O_2 on these supported gold T and P clusters, at various doping concentrations. This is done using the technique of constrained minimization, with the O–O distance as the reaction coordinate. As an example of results from one such set of calculations, in Fig. 2, we show how the total energy of the system varies with the O–O bond length for adsorption initially in the P2 geometry, for a dopant concentration of 2.78%.

On the pristine substrate, where the T morphology is lower in energy than P, we obtain $E_{\text{diss}} = 0.68$ eV for the adsorption geometry T1. Upon doping, the P morphology becomes lower in energy than T. Interestingly, we find that not

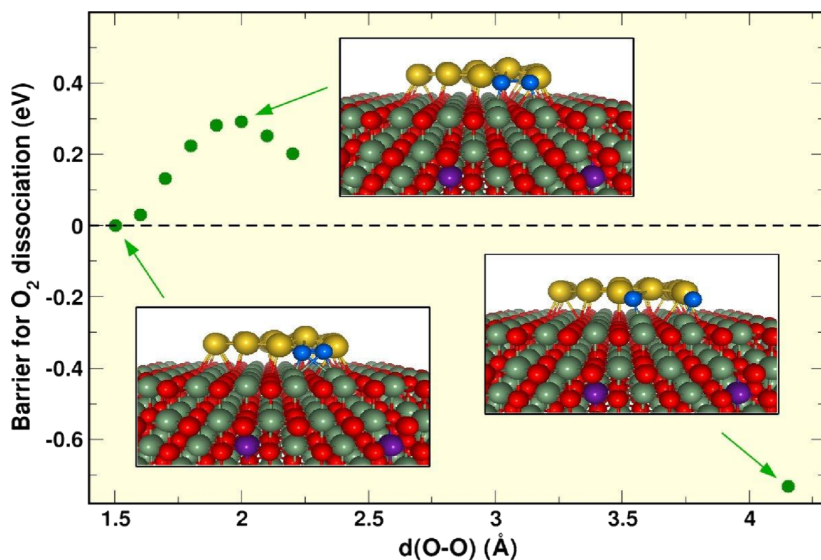


FIG. 2. Example of a computation of a dissociation barrier: results for total energy versus O–O bond length for adsorption geometry P2 on 2.78% Al-doped MgO. The insets depict the system geometry at various stages of the reaction. Gray, purple, and yellow spheres represent Mg, Al, and Au atoms, respectively. O atoms in the substrate/adsorbed on the surface are red/blue.

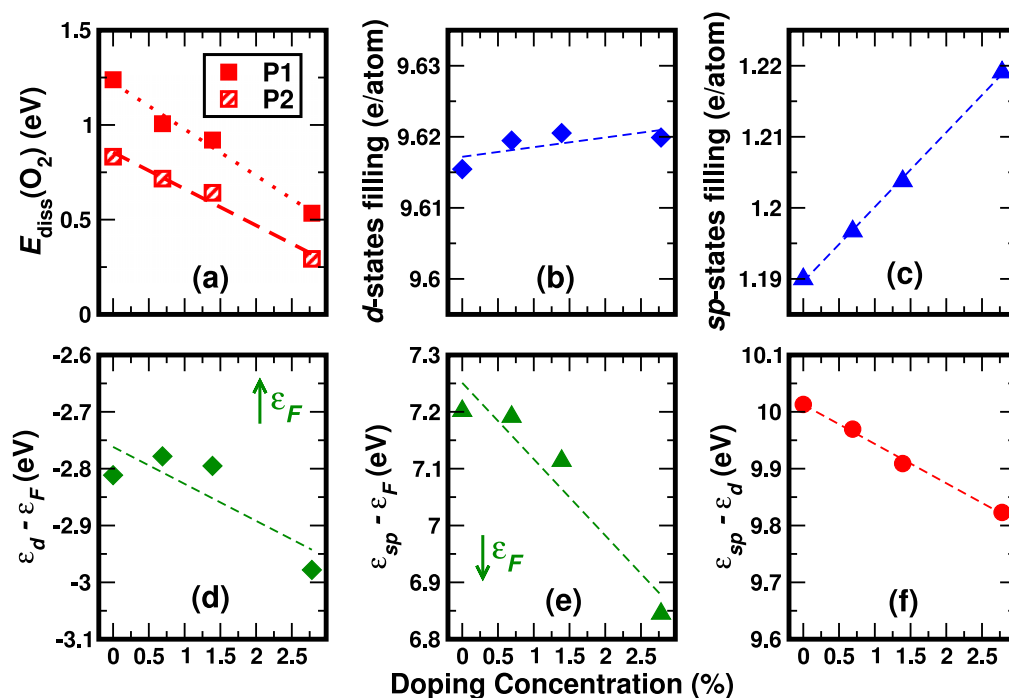


FIG. 3. (a) The barrier for O_2 dissociation for the P1 and P2 geometries of the Au(P) cluster, (b) the filling in the Au d -states, (c) the filling in the Au sp -states, both averaged over all atoms in the cluster, (d) the position of the d -band center, ϵ_d , (e) the center of the sp -bands, ϵ_{sp} , and (f) $\epsilon_{sp} - \epsilon_d$, all as a function of doping concentration. The arrows in (d) and (e) show the direction of the Fermi energy.

only do we obtain significantly lower dissociation barriers for P geometries on the doped substrates, but it is also possible to tune E_{diss} by varying the doping concentration. This is shown in Fig. 3(a): for both adsorption geometries P1 and P2 on the planar cluster, we find a very dramatic decrease of E_{diss} upon doping; the greater the doping, the lower the barrier. For P2, E_{diss} is lowered from 0.83 eV on undoped MgO to 0.29 eV at a doping concentration of 2.78%, a reduction by 65%. Perhaps more meaningfully, this represents a decrease of 57% with respect to $E_{\text{diss}} = 0.68$ eV, the value for the T1 adsorption geometry on the pristine substrate. Since reaction rate constants vary exponentially with E_{diss} , this corresponds to a speeding up of the dissociation rate by five orders of magnitude at room temperature (assuming that the pre-exponential factors remain the same). As we had found earlier for the energetics of the morphology change,¹¹ here too we find that varying the position of the dopant atom (either laterally or vertically) has only a small effect on dissociation barriers. For example, for a doping concentration of 2.78%, moving the dopant atom from the third substrate layer to the second substrate layer changes the dissociation barrier at P1 from 0.53 eV to 0.55 eV.

We find that the adsorption energy per oxygen atom after dissociation is 0.76 eV for the P1 site, and 0.71 eV for the P2 site (both at a doping concentration of 2.78%). This falls into the intermediate range of binding energies desirable for the reaction to be favorable.⁴

For the T cluster, a similar reduction of barriers upon doping is observed: we find that the barrier for O_2 dissociation is lowered from 0.68 eV to 0.39 eV when the dopant concentration is 2.78%. Note, however, that at this dopant concentration, the T morphology is not energetically favored, since the P form is lower in energy on the doped substrate.

On examining our results for barriers, we conclude that the dramatic lowering of barriers is caused primarily by increasing the charge transfer to the cluster by increasing the dopant concentration, rather than due to the change in cluster morphology.

We now attempt to understand and explain our results. We first examine trends in charge transfer and the activation of the O–O bond, at the P1 and P2 sites. Fig. 4(a) shows the charge gained by the O_2 molecule upon adsorption on the planar Au_{20} cluster, while Fig. 4(b) shows the resulting increase in the O–O bond length. As expected, upon adsorption, the molecule gains charge, and the interatomic length is increased with respect to the gas phase value of 1.21 Å, which will aid dissociation. However, one sees a clear difference between the trends at the two sites P1 and P2. At P1, the charge transferred to the molecule increases monotonically with the doping concentration, going from 0.53 e to 1.20 e over the range of doping concentrations considered. Correlating with this, there is a significant linear increase in the O–O bond length, from 1.32 Å to 1.50 Å. However, at the P2 site, the changes in charge transfer and bond activation are much smaller and not even monotonic. Since the O_2 dissociation energy decreased monotonically and significantly at both the P1 and P2 sites [recall Fig. 3(a)], this suggests that we need to look further in order to explain satisfactorily the observed trends in dissociation energy as a function of substrate doping.

Accordingly, we now examine how the electronic structure of the Au cluster changes upon doping the substrate. The “ d -band model” of catalysis³⁰ has been extremely successful for transition metal catalysts with partially filled d states. However, it has also been used to explain why gold is the noblest metal in extended systems,³¹ and why gold becomes reactive in nanometer sizes when the coordination number is

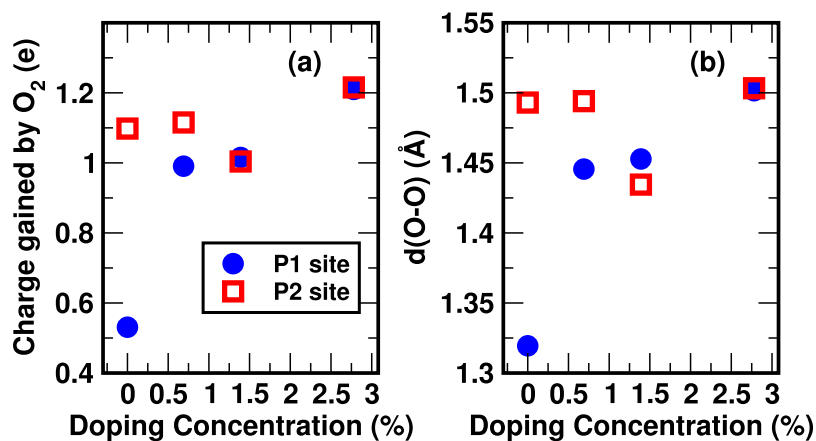


FIG. 4. Trends in charge transfer and activation for oxygen on planar Au₂₀/MgO: (a) the charge transferred to the O₂ molecule from the substrate or cluster, (b) the elongation of the O–O bond in the adsorbed O₂ molecule for the two adsorption sites P1 and P2 in the planar Au₂₀ cluster as a function of substrate doping concentration.

lowered.^{32,33} In this model, one considers a parameter called the “*d*-band center,” ϵ_d , which is the weighted center of the *d*-band density of states, relative to the Fermi energy ϵ_F . The basic statement of the *d*-band model is that the higher in energy ϵ_d is, the better the catalyst.

However, the *d*-band model, in its original simple form, where all the “action” is in the *d* electrons alone, and the remaining electrons behave in the same way in all situations, cannot be used to explain the increase in reactivity on substrate doping that we observe, as we now demonstrate. Let us first examine how the filling of the various electronic states of the Au cluster changes when the substrate is doped with an electron donor. Unlike in an isolated Au atom, in Au₂₀ on pristine MgO, the *d* states are only partially occupied: out of 11 valence electrons, on average 9.63 and 9.62 are in *d* states in the T and P geometries, respectively. This is in agreement with previous experimental findings about the distribution of electrons in *s*, *p*, and *d* states in small Au clusters.³⁴ However, upon introducing additional electrons by doping the substrate up to a level of 2.78%, only 0.09 electrons go into the *d* states of Au₂₀, whereas 0.58 electrons go into the *s* and *p* states [see Figs. 3(b) and 3(c)]. This rather large uptake of electrons can be explained by the high electronegativity of Au atoms, which is further increased due to relativistic effects.^{35,36} As a result of this large electron transfer from the doped substrate to the Au cluster, the *d*-band center of Au moves down in energy, (i.e., opposite the direction one would expect if the *d*-band model could explain the observed lowering of barriers), and so does the *sp*-band center, ϵ_{sp} . This is shown in Figs. 3(d) and 3(e), and the reason for this is shown in the cartoon model in Fig. 5. Note that the downward shift in ϵ_{sp} is greater than the downward shift in ϵ_d , primarily because of the greater injection of electrons into the *sp* states. Note also that to characterize the shifts in energy of the *sp* bands, we have chosen to look at a single energy ϵ_{sp} , defined as the energy where these states achieve half-filling (see the supplementary material for definitions of band centers as well as results for their behavior when they are referenced to the vacuum level instead of the Fermi level).⁴³

Within the *d*-band model, the energy of the transition state for the dissociation process can be estimated as³⁷

$$\delta E_{ts} \sim -\frac{2V^2}{\epsilon_{a'} - \epsilon_d} + \alpha V^2, \quad (1)$$

where $\epsilon_{a'}$ is the energy of the molecular antibonding state after having been renormalized by interacting with the metal’s *s*- and *p*-bands, V is the coupling matrix element between the molecular orbitals and the *d* states of gold, and α is the proportionality constant that is involved in the orthogonalization term.

We can now extend the *d*-band model to incorporate the changes in the behavior of *sp* electrons upon substrate doping, by writing

$$\delta E_{ts} \sim -\frac{2V^2}{\epsilon_{sp} - \epsilon_d - \delta} + \alpha V^2, \quad (2)$$

where δ is approximately a constant (see the supplementary material).⁴³

This suggests that $\Delta\epsilon \equiv \epsilon_{sp} - \epsilon_d$ should be a good descriptor of the catalytic activity of gold clusters and should be small for a good catalyst. In tuning catalytic activity using the *d*-band model, one focuses on making $\epsilon_{a'} - \epsilon_d$ or $\Delta\epsilon$ small by pushing up ϵ_d ; in systems like ours, one instead reduces $\Delta\epsilon$ by lowering ϵ_{sp} . Like the *d*-band center, $\epsilon_{sp} - \epsilon_d$ has the advantage that it is easily computed and is a property of the catalyst alone. One question that arises in this field is whether it is more appropriate to reference computed energies to the

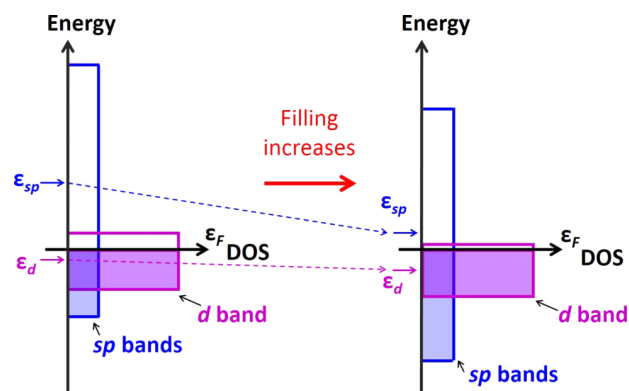


FIG. 5. Cartoon model showing the densities of states (DOS) of the *sp*- and *d*-bands, and the downshift in energies of both upon an increase in filling. The downward shift is more for the *sp*-bands than the *d*-band because of both the larger injection of charge and the shape of the DOS. ϵ_{sp} , ϵ_d , and ϵ_F are the *sp*-band center, *d*-band center, and Fermi energy, respectively. Note that this figure is schematic only, and in reality the Au *d* DOS is far from rectangular, with a peak well below ϵ_F , and a tail extending to higher energies.

Fermi energy or the vacuum energy; note that $\epsilon_{sp} - \epsilon_d$ also has the additional advantage that it is independent of any choice of reference energy.

In Fig. 3(f), we examine how $\Delta\epsilon$, the difference in the energies of the sp - and d -states, varies with doping. One sees that indeed, $\Delta\epsilon$ decreases upon doping the substrate. This figure finally contains the key to explaining our results in Fig. 3(a): the progressive lowering of the denominator in the first term on the right-hand-side of Eq. (1) or Eq. (2), due primarily to the downshift in energies of the s and p electrons, is responsible for the lowering of barriers with doping.

Similar arguments should presumably hold also for other sizes of gold clusters, on other oxide substrates, other dopant atoms, and other charging mechanisms that add electrons to the cluster. A number of studies have shown that negatively charging gold clusters has a significant activity on their catalytic activity.^{5,19,38–41} In such scenarios, mechanisms similar to those described above would presumably operate, and it would be interesting to re-examine these cases in this light, to see if this can explain the changes in reactivity in these situations. The arguments presented in this paper apply to negatively charged Au clusters; and we note that the behavior of s electrons has also been invoked to explain the enhanced reactivity for partial oxidation of methane of positively charged Au clusters in the gas phase and on an undoped oxide substrate.⁴²

In this study, we have used Al-doped MgO as the substrate, because it presents itself as a very simple system to model the effects of doping by an electron donor. However, we note that for actual practical applications, doping by a simple metal like Al may not be the best choice, as the excess charge may be trapped at impurity sites; a better choice may be to use a transition metal with variable oxidation state as the dopant atom.^{12,13}

We note that another demonstration of the possibilities offered by substrate doping has been furnished by other authors who have studied gold clusters on doped ceria substrates;¹⁰ the focus of their work is somewhat different from ours, in that they have examined how the presence of the dopants affects the vacancy formation energy, which in turn serves as a good reactivity descriptor for CO oxidation in the combined system.

In summary, we have shown, by theoretical calculations, that the strategy of substrate doping that was recently proposed as a method of tuning the morphology of gold clusters on oxide substrates, and that has been shown to work for this purpose both theoretically and experimentally,^{11–13} confers in addition the highly desirable benefit of drastically reducing barriers for oxygen dissociation on these clusters, so that reaction rates are significantly increased. The general nature of our arguments suggests that this should hold true also for several other reactions. We hope the work presented here will stimulate experimental measurements of reactivity on such doped systems. This work underlines the importance of nanoparticle-substrate interactions in nanocatalysis. The analysis presented shows that rather than the d -electrons, which have been cited as the source of the enhanced catalytic activity of small gold nanoparticles,³² it is the s and p electrons of gold whose energies and electronic structure play a key

role in the reduction of reaction barriers, in this case. We believe that an appropriate descriptor of the reactivity of gold nanoparticles could be $\epsilon_{sp} - \epsilon_d$, the difference in energies of the sp and d states.

The authors acknowledge support from the Indo-Italian POC in Science and Technology of the DST, India, and the MAE, Italy, and also the ICMS-SISSA Exchange Programme. Computational Facilities were provided by TUE-CMS, JNCASR; and CINECA. We thank Ram Seshadri, Rajdeep Banerjee, and Sukanya Ghosh for helpful discussions. S.N. acknowledges the Sheikh Saqr Laboratory of the International Centre for Materials Science, JNCASR.

¹M. Haruta, *Catal. Today* **36**, 153 (1997).

²G. C. Bond and D. T. Thompson, *Gold Bull.* **33**, 41 (2000).

³T. Bernhardt, U. Heiz, and U. Landman, in *Nanocatalysis*, Nanoscience and Technology edited by U. Heiz and U. Landman (Springer, Berlin, Heidelberg, 2007), pp. 1–191.

⁴H. Falsig, B. Hvolbæk, I. Kristensen, T. Jiang, T. Bligaard, C. Christensen, and J. Nørskov, *Angew. Chem., Int. Ed.* **47**, 4835 (2008).

⁵A. Sanchez, S. Abbet, U. Heiz, W.-D. Schneider, H. Hakkinen, R. N. Barnett, and U. Landman, *J. Phys. Chem. A* **103**, 9573 (1999).

⁶N. Nikbin, N. Austin, D. G. Vlachos, M. Stamatakis, and G. Mpourmpakis, *Catal. Sci. Technol.* **5**, 134 (2015).

⁷M. Stamatakis, M. A. Christiansen, D. G. Vlachos, and G. Mpourmpakis, *Nano Lett.* **12**, 3621 (2012).

⁸P. Ghosh, M. Farnesi Camellone, and S. Fabris, *J. Phys. Chem. Lett.* **4**, 2256 (2013).

⁹P. Schwerdtfeger, *Angew. Chem., Int. Ed.* **42**, 1892 (2003).

¹⁰H. Y. Kim and G. Henkelman, *J. Phys. Chem. Lett.* **3**, 2194 (2012).

¹¹N. Mammen, S. Narasimhan, and S. de Gironcoli, *J. Am. Chem. Soc.* **133**, 2801 (2011).

¹²X. Shao, S. Prada, L. Giordano, G. Pacchioni, N. Nilius, and H.-J. Freund, *Angew. Chem., Int. Ed.* **50**, 11525 (2011).

¹³F. Stavale, X. Shao, N. Nilius, H.-J. Freund, S. Prada, L. Giordano, and G. Pacchioni, *J. Am. Chem. Soc.* **134**, 11380 (2012).

¹⁴D. Ricci, A. Bongiorno, G. Pacchioni, and U. Landman, *Phys. Rev. Lett.* **97**, 036106 (2006).

¹⁵C. Zhang, B. Yoon, and U. Landman, *J. Am. Chem. Soc.* **129**, 2228 (2007).

¹⁶C. Harding, V. Habibpour, S. Kunz, A. N.-S. Farnbacher, U. Heiz, B. Yoon, and U. Landman, *J. Am. Chem. Soc.* **131**, 538 (2009).

¹⁷M. Sterrer, T. Risse, M. Heyde, H.-P. Rust, and H.-J. Freund, *Phys. Rev. Lett.* **98**, 206103 (2007).

¹⁸B. Yoon and U. Landman, *Phys. Rev. Lett.* **100**, 056102 (2008).

¹⁹L. Molina and B. Hammer, *J. Catal.* **233**, 399 (2005).

²⁰M. A. Pedrosa, R. Pareja, R. Gonzalez, and M. M. Abraham, *J. Appl. Phys.* **62**, 429 (1987).

²¹R. Gonzalez, Y. Chen, and K. L. Tsang, *Phys. Rev. B* **26**, 4637 (1982).

²²J. Andersin, J. Nevalaita, K. Honkala, and H. Häkkinen, *Angew. Chem., Int. Ed.* **52**, 1424 (2013).

²³S. S. Yamijala, A. Bandyopadhyay, and S. K. Pati, *J. Phys. Chem. C* **118**, 17890 (2014).

²⁴K. Mondal, C. Kamal, A. Banerjee, A. Chakrabarti, and T. K. Ghanty, *J. Phys. Chem. C* **119**, 3192 (2015).

²⁵P. Giannozzi, S. Baroni, N. Bonini, M. Calandra, R. Car, C. Cavazzoni, D. Ceresoli, G. L. Chiarotti, M. Cococcioni, I. Dabo, A. D. Corso, S. de Gironcoli, S. Fabris, G. Fratesi, R. Gebauer, U. Gerstmann, C. Gougoussis, A. Kokalj, M. Lazzeri, L. Martin-Samos, N. Marzari, F. Mauri, R. Mazzarello, S. Paolini, A. Pasquarello, L. Paulatto, C. Sbraccia, S. Scandolo, G. Sclauzero, A. P. Seitsonen, A. Smogunov, P. Umari, and R. M. Wentzcovitch, *J. Phys. Condens. Matter* **21**, 395502 (2009).

²⁶D. Vanderbilt, *Phys. Rev. B* **41**, 7892 (1990).

²⁷J. P. Perdew, *Electronic Structure of Solids* (Akademik Verlag, Berlin, 1991).

²⁸L. M. Molina and B. Hammer, *Phys. Rev. B* **69**, 155424 (2004).

²⁹P. Frondelius, H. Häkkinen, and K. Honkala, *Angew. Chem., Int. Ed.* **49**, 7913 (2010).

³⁰B. Hammer and J. Nørskov, in *Impact of Surface Science on Catalysis*, Advances in Catalysis edited by B. C. Gates and H. Knozinger (Academic Press, 2000), Vol. 45, pp. 71–129.

³¹B. Hammer and J. K. Nørskov, *Nature* **376**, 238 (1995).

- ³²N. Lopez, T. Janssens, B. Clausen, Y. Xu, M. Mavrikakis, T. Bligaard, and J. Nørskov, *J. Catal.* **223**, 232 (2004).
- ³³M.-S. Miao, J. A. Kurzman, N. Mammen, S. Narasimhan, and R. Seshadri, *Inorg. Chem.* **51**, 7569 (2012).
- ³⁴J. A. van Bokhoven and J. T. Miller, *J. Phys. Chem. C* **111**, 9245 (2007).
- ³⁵P. Schwerdtfeger, *Chem. Phys. Lett.* **183**, 457 (1991).
- ³⁶P. Schwerdtfeger, *Heteroat. Chem.* **13**, 578 (2002).
- ³⁷B. Hammer and J. Nørskov, *Surf. Sci.* **343**, 211 (1995).
- ³⁸B. Yoon, H. Häkkinen, and U. Landman, *J. Phys. Chem. A* **107**, 4066 (2003).
- ³⁹Q. Sun, P. Jena, Y. D. Kim, M. Fischer, and G. Gantefor, *J. Chem. Phys.* **120**, 6510 (2004).
- ⁴⁰B. Yoon, H. Häkkinen, U. Landman, A. S. Wörz, J.-M. Antonietti, S. Abbet, K. Judai, and U. Heiz, *Science* **307**, 403 (2005).
- ⁴¹A. Roldan, J. M. Ricart, F. Illas, and G. Pacchioni, *Phys. Chem. Chem. Phys.* **12**, 10723 (2010).
- ⁴²D. J. Mowbray, A. Migani, G. Walther, D. M. Cardamone, and A. Rubio, *J. Phys. Chem. Lett.* **4**, 3006 (2013).
- ⁴³See supplementary material at <http://dx.doi.org/10.1063/1.4932944> for equations defining the d -band center, ϵ_d , and the sp -band center, ϵ_{sp} , behavior of ϵ_d and ϵ_{sp} as a function of doping concentration, when referenced to the vacuum level, and data supporting the introduction of Eq. (2).